Hindawi
Journal of Engineering
Volume 2023, Article ID 8081874, 19 pages
https://doi.org/10.1155/2023/8081874

Research Article

Studying the Synergetic Effect of Point-Extraction and Longitudinal Ventilation on the Maximum Smoke Temperature and Back-Layering Length in Tunnel Fires

Ebrahim Barati and Seyyed Omid Haghani

Mechanical Engineering Department, Khayyam University, Mashhad, Iran

Correspondence should be addressed to Ebrahim Barati; barati.ebrahim@gmail.com

Received 16 March 2023; Revised 4 May 2023; Accepted 1 August 2023; Published 14 August 2023

Academic Editor: Hongfu Zhang

This study investigates the impact of combining longitudinal and point-extraction ventilated systems on temperature distribution and back-layering length in tunnel fires. Numerical simulations are conducted using a fire dynamic simulator (FDS), and reduced-scale tunnel fire experiments with a scale of 1/10 are introduced to provide supplementary data. Results indicate that the longitudinal velocity is more critical than other factors in reducing the highest temperature and casualties. Lowering the temperature below the tunnel ceiling is not caused by increasing the ceiling extraction velocity. Additionally, the study reveals that the fire source-ceiling distance and their relative positions play a crucial role in temperature distribution and plug-holing phenomenon in the tunnel. By using the Taguchi method, it is determined that a fire at a height of 0.125 m has a maximum ceiling temperature of 1.8, 1.3, and 1.1 times when the fire source happens on the floor with longitudinal velocities of 0.133, 0.265, and 0.53 m/s, respectively. The extraction point has diverse effects provided that the longitudinal ventilation velocity is set by critical velocity. The study's objective is to provide tunnel engineering managers with a correlation to predict the highest temperature, which is a vital parameter for emergency evacuation. In conclusion, this study highlights the importance of considering longitudinal and point-extraction ventilated systems and their relative speeds in reducing the severity of tunnel fires.

1. Introduction

In recent times, the growth of road tunnel networks around the world has resulted in a rise in the possibility of tunnel fires, increasing the risk of death and destruction of assets and posing excessive hazards to human life. The study of a fire in a tunnel is an important subject regarding the safety of the tunnel [1–3]; therefore, considering a development of the smoke temperature close to the ceiling is an important aspect that must be considered. Due to limited space and inadequate exits, fire normally occurs in tunnels when a significant amount of hot smoke is accumulated in the tunnel as a result of the fire [4, 5]. Because of the high temperatures and the limited visibility, it can be a dangerous place for people. Tunnel disasters have caused difficulties for emergency evacuation, and performant smoke control is an elemental need in a tunnel fire. Designing a practical smoke control program is essential to preclude possible fires in a tunnel. Ventilation systems and smoke control policies must guarantee that people in the tunnel can escape harmlessly under smoke peril [6–8]. Assorted smoke control systems are grown for smoke extraction when a fire disaster starts. Longitudinal extraction system and point-extraction system (PES) are the utmost frequently approved procedures in road tunnels [9]. For longitudinal extraction strategies, a jet fan on the top of the tunnel generates the longitudinal flow and is capable of managing the flow towards the exit.

Many preceding numerical and experimental investigations on the ventilation of the tunnel, in the case of fire incidence, have been carried out [10–12]. Song et al. [13] studied the various smoke extraction accomplishment in a tunnel with 100 MW heat release rate. They concluded that

extracting smoke with a single point is more beneficial compared to devising several extracting points under celling. A computational fluid dynamics simulation means to explore that the optimum rate of exhaust flow was employed by Lin and Chuah [14], and Yoon et al. [15] studied numerically the practicability of the point-extraction system policies in a large cross-section tunnel. The smoke back-layer length and its width in tunnel fires with the single-point and multipoint extractions were obtained by Zhu et al. [16]. Mei et al. [17] carried out several computer simulations; they analyzed the smoke temperature and the area of visibility to assess the efficacy of the point-extraction system (PES). They found that the evacuation can be slightly affected by the transfer location fire. In addition, a model was developed by Yan and Zhang [18] to quantify the smoke back-layering length in tunnel fires using longitudinal velocity and point-extraction system.

Studies by Wang et al. [19], Jiang et al. [20], and Tang et al. [21] have focused on the flow patterns, back-layering length of smoke, and temperature distribution in tunnel fires with various extraction systems. The point-extraction system is considered a practical solution to manage tunnel fires, and research has been conducted on the extreme temperatures under different situations, including natural smoke exhaustion, inclined tunnels, blockage influence, and various fire locations [22–29]. Recently, the use of accompanying ventilation schemes, combining longitudinal ventilation with a single-vent system, has become more common in road tunnels [30]. However, limited research has been conducted on the temperature distribution when a conventional ventilation system is supported by a vent system. This research aims to explore the smoke temperature, thermal back-layering length, and plug-holing phenomenon under the influence of point-extraction system and longitudinal ventilation, using the Taguchi method to manipulate essential factors such as ceiling extraction velocity or longitudinal ventilation velocity.

The primary innovation of this study is to reduce the highest temperature of the tunnel during a fire and improve the understanding of smoke performance to find an appropriate smoke control approach for safe evacuation under various fire situations. By combining longitudinal and point-extraction ventilated systems, this study aims to provide insight into the impact of different ventilation velocities and fire source-ceiling distances on the severity of tunnel fires. The results of this study can be used by tunnel engineering managers to predict the highest temperature and plan emergency evacuation procedures accordingly. Ultimately, this research aims to contribute to the development of more efficient and effective smoke control strategies for tunnel fires.

2. Problem Statement and Physical Description

This paper analyses a numerical simulation based on Navier–Stokes equations achieved by using the Fire Dynamics Simulator (FDS 6.6). This software offers the capability of solving a mathematical approximation of the Navier–Stokes equations numerically for a low Mach number, thermally driven flow with an emphasis on the transport of smoke and heat from fires. It is necessary to use the large eddy simulation (LES) method in order to predict the turbulence and buoyancy of a fluid flow. As a result of the use of this method, a number of studies have been conducted in the fields of fire safety and fire prevention. In order to visualize the dispersion of smoke particles in the tunnel fires as well as the velocity field in the tunnel fires during construction, we used Smokeview and Tecplot.

2.1. Physical Description of the Tunnel Model. The numerical modeling is performed in a tunnel model with dimensions of $0.25 \times 0.25 \times 12$ m. In the context of a tunnel fire, an intentional ignition source in the form of a burner is employed to initiate and sustain the fire within the tunnel. The dimension of the squared burner is 0.1 m, acting as a fire, to release heat continuously, and the vent is placed 0, 1, and 3 m away from the upstream and downstream of the burner. The size of the vent is 0.1×0.1 mounted at the central of the ceiling. The burner is centrally positioned within the tunnel, and the length of back-layering is restrained through the synergistic interaction of the ventilation system and the upstream and downstream vent systems adjacent to the fire source. All simulations are conducted for 5 kW heat release rate with the four levels of vent vertical velocities: 0 m/s, 1 m/s, 2 m/s, and 3 m/s, and three levels of longitudinal ventilation velocities: 0.133 m/s, 0.265 m/s, and 0.53 m/s. The ambient temperature is considered 20°C.

3. Numerical Model

The computing power maturity and the extension of numerical modeling have directed investigators to the CFD applied to a fire modeling. The numerical model is constructed by Fire Dynamic Simulator. The Fire Dynamics Simulator (FDS) has been advanced at NIST to explore fire behavior and to analyze the efficiency of fire protection systems. Simulation of fire-driven flow can be conducted in FDS by employing the LES turbulence model. FDS has been extensively utilized in the exploration of smoke behavior, and it is validated broadly. The numerical solution of the governing equations, specifically the Navier–Stokes equations and the energy equations, is performed within the Fire Dynamics Simulator software package, employing advanced numerical methods for accurate and efficient computations. It is worth mentioning that the FDS code numerically solves a special form of Navier–Stokes equations for low Mach flows. Current derivatives in the equations of conservation of mass, momentum, and energy are discretized using the finite difference method with second-order accuracy and are solved explicitly in time. However, the phenomenon of radiation is calculated using the control volume method.

To have reasonable accuracy, mesh refining is performed. In the FDS code, the following equations will be solved numerically:

$$\frac{\partial \rho}{\partial t} + \nabla . \rho u = 0. \tag{1}$$

By applying the law of conservation of mass to a differential element of the fluid, the overall mass conservation equation will be obtained as equation (1). In this equation, ρ and u represent density and velocity.

$$\frac{\partial}{\partial t}\left(\rho Y_\alpha\right) + \nabla.\left(\rho Y_\alpha u\right) = \nabla.\left(\rho D_\alpha \nabla Y_\alpha\right) + \dot{m}_\alpha'''. \quad (2)$$

Equation (2) is related to the mass constancy of the species. Fick's law states that in a two-component mixture, the mass flux of α type is obtained from the following equation: $\dot{m}_\alpha'' = Y_\alpha \dot{m}_{\text{tot}}'' - \rho D_{\alpha\beta}\nabla Y_\alpha$. Therefore, assuming that Fick's law is correct in multicomponent mixtures, the general form of the equation of the mass of the species will be equation (2). In this regard, term $\dot{m}_\alpha'''$ is the rate of production or consumption of species α.

$$\frac{\partial}{\partial t}(\rho u) + \nabla.(\rho u u) + \nabla P = \rho g + f_b + \nabla.\tau_{ij}. \quad (3)$$

By applying Newton's second law on a differential element of fluid, the equation of conservation of momentum will be obtained as equation (3). In this equation, u is the velocity vector, f_b is the external force, and τ_{ij} is the stress tensor for Newtonian fluids.

$$\frac{\partial}{\partial t}\left(\rho h_s\right) + \nabla.\left(\rho h_s u\right) = \frac{DP}{Dt} + \dot{q}''' - \nabla.\dot{q}'' + \varepsilon. \quad (4)$$

Equations of energy conservation based on sensible enthalpy will be obtained by applying the first law of thermodynamics to a differential element of fluid in the form of equation (4), where h_s represents the sensible enthalpy of the fluid, which is a function of temperature, and ε represents the decay term in the energy equation. $\dot{q}'''$ is the rate of heat released per unit volume by chemical reaction and $\dot{q}''$ shows the rate of heat transfer through radiation and conduction. The FDS user guide proposes a nondimensional expression of $D^* = (Q/\rho T C_p \sqrt{g})^{0.4}$ for assessing a mesh resolution with D^*. The recommended value of $D^*/\delta x$ is in the range of 4–16. In this investigation, fire grid numbers are studied to confirm that the results are grid independent. In the context of FDS 6.6 fire numerical simulations in a tunnel, grid independence assumes paramount importance to ascertain the credibility and precision of the results. In this work, the investigation into the results' independence on the grid number substantiates that the mesh resolution does not significantly impinge upon the reliability of the outcomes.

4. Results and Discussion

Figure 1 shows the meshing used in the FDS 6.7 code. Along with the numerical simulations described in the next section, other simulations are conducted with the precise target of verifying the model validity, by examining the agreement between experimental results and model predictions. Figure 2 illustrates the variation of critical velocity with heat release rate (HRR) and a remarkable agreement is observed, and the simulation is compared with the study by Li et al. [31] and Wu and Bakar [32]. Presented in this study are simulations of reduced-scale tunnel fire experiments, utilizing a scale of 1/10. It is worth noting that previous research conducted by Wu and Bakar has confirmed the reliability of reduced-scale simulations, making them a viable option for further experimentation [33]. As a result, this study employs the reduced scale for the remaining

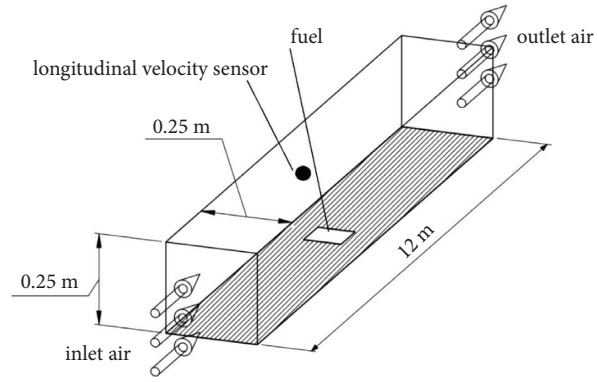

Figure 1: Concerned geometry and its boundary.

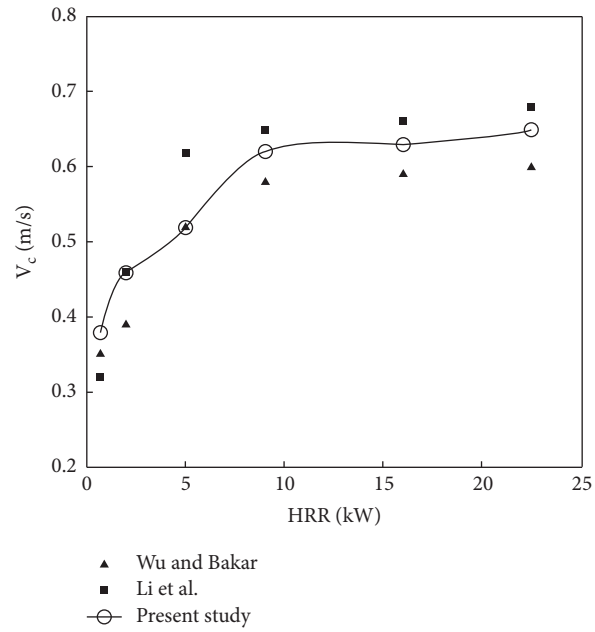

Figure 2: Variation of critical velocity with HRR.

simulations, allowing for significant computational time savings while maintaining accuracy.

Once a fire occurs, an exhaust fan close to the fire source should be turned on to preserve the smoke at the top of the tunnel; then, the exhaust fan can extract the smoke. Simultaneous operation of the longitudinal ventilation and point-extraction system has apparent benefits in the case of traffic jams and fire situations; thus, activating both the systems should be considered. A fan, placed at the entrance of tunnel, is capable of generating velocity longitudinally, while exiting from opposite side. The vertical extraction flow is generated with the aid of fan fixed on the ceiling. Adjustment to various speeds is possible to provide the necessary flow rate. In the numerical simulation, there are three different longitudinal ventilation velocities: 0.133, 0.265, and 0.53 m/s, and four ceiling extraction velocities: 0, 1, 2, and 3 m/s.

A huge temperature can be a tremendous hazard to the people in an incidence of fire when the ventilation system is not designed correctly. All emergency evacuation plans

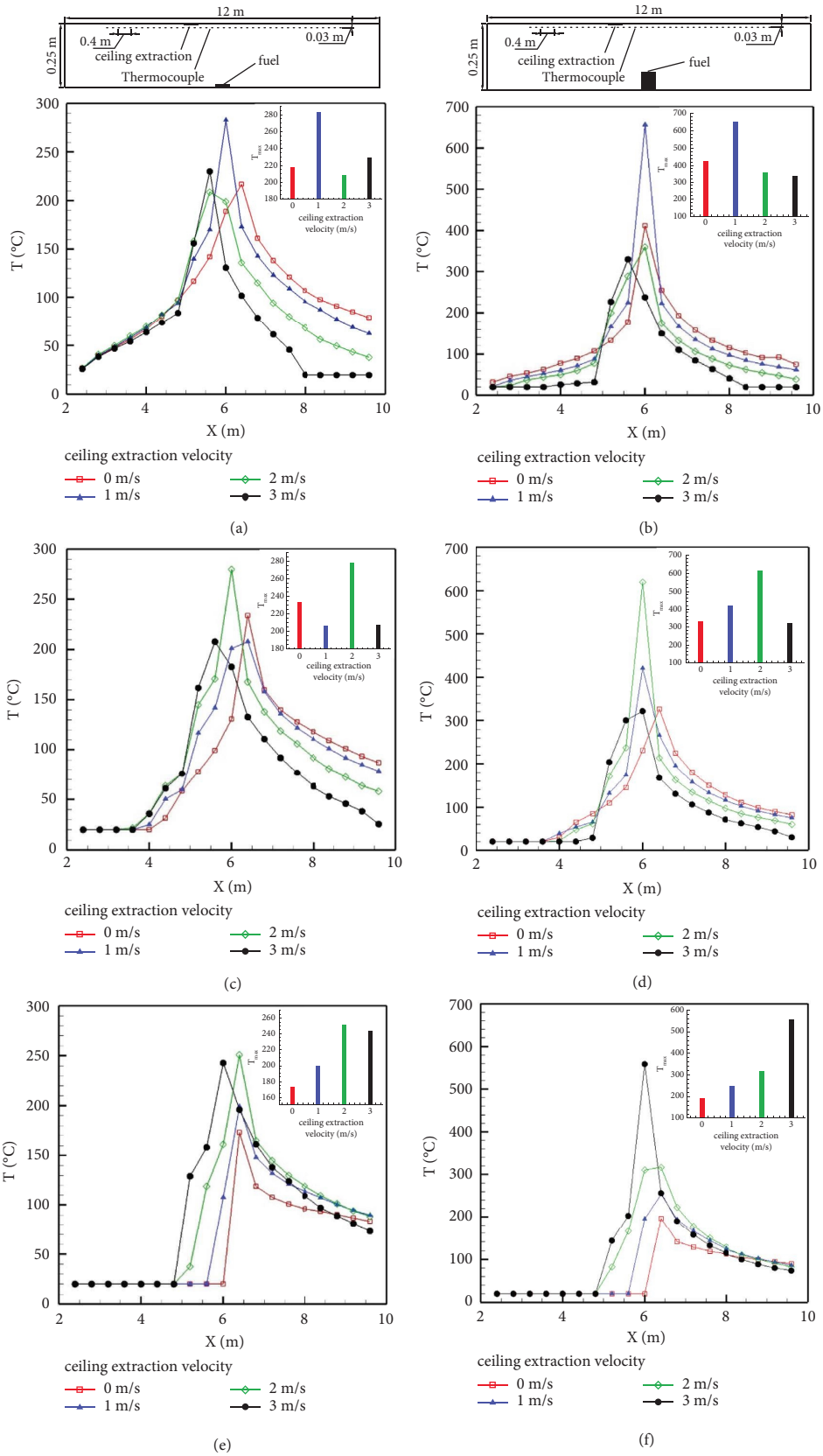

Figure 3: Ceiling temperature distribution through the tunnel ventilated longitudinally and vertically (HRR = 5 kW with various L.V.). (a) L.V. = 0.133 m/s. (b) L.V. = 0.133 m/s. (c) L.V. = 0.265 m/s. (d) L.V. = 0.265 m/s. (e) L.V. = 0.53 m/s. (f) L.V. = 0.53 m/s.

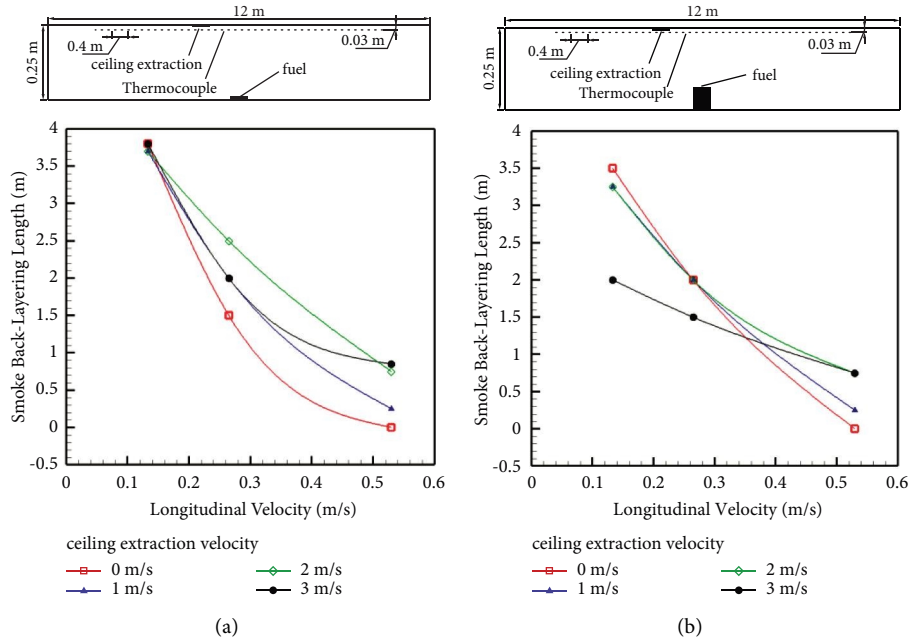

Figure 4: The variation of back-layering flow length with vertical extraction velocity (HRR = 5 kW, L.V. = 0.53 m/s, and E.V. = 3 m/s).

should secure the domain in the upstream area of the tunnel at a bearable temperature. To research the temperature distribution in the reduced-scale tunnel, the ceiling temperature is determined to preserve an acceptable condition in the tunnel area from the fire incident; it is vital to consider the required minimum longitudinal flow velocity, thereby preventing smoke back-layering. For the present work with HRR = 5 kW, the critical velocity is 0.53 m/s when ceiling extraction is 0 m/s. Figure 3 displays the smoke temperature distribution under the ceiling with varied ceiling smoke extraction velocities and various longitudinal velocities. From Figure 3, it is obvious that for E.V. = 0, the maximum smoke temperature is 215, 230, and 170 when longitudinal ventilation velocity varies from 0.133, 0.256, and 0.53 m/s, respectively, when the fire is on the floor. As fire occurs at the height of 0.125 m, the temperature increases rapidly. Figure 3 illustrates that the temperature of smoke near the tunnel ceiling predominantly increases with an increase in ceiling extraction velocity and subsequently reduces with the increment of mass flow rate. It is worth mentioning that the ceiling smoke extraction sucks in heat and smoke. Therefore, the stack effect occurs when the velocity of extraction is relatively low during the growth period. It can be seen that when the extraction point is placed 1 m upstream side of the fire source, the extraction velocity has different effects on the temperature distribution. For a critical longitudinal velocity (L.V. = 0.53 and E.V. = 0), the extraction has diverse effects, thereby being responsible for experiencing the higher temperature distribution. Moreover, the fire source-ceiling height has remarkable effects on a maximum temperature. According to Figures 3(e) and 3(f), the maximum temperature differences for various extraction velocities are significant, with a difference of 50 and 250 observed for fire source-ceiling heights of 0.25 and 0.125 m, respectively. These findings emphasize the crucial role of fire source height in determining maximum temperature, which has significant implications for smoke layer thickness and plug-holing occurrence. In light of these relationships, understanding the interplay between fire source height and these variables is critical for effective tunnel fire management and the development of future safety measures.

Figure 4 displays the importance of longitudinal flow rate to control the thermal back-layering length. In the condition of longitudinal ventilation, the hot smoke generated by the fire is mainly blown downstream of the fire source; when the velocity of longitudinal ventilation is not enough to control the flow of the hot smoke, some smoke will spread upstream to form the smoke lack-layering. It is observed that increasing the longitudinal velocity results in a reduction of the thermal back-layering length. From Figure 4, it is clear that the longest thermal back-layering is corresponded to L.V. = 0.131 m/s. Vent system is regularly utilized to govern the smoke dispersion in a ventilation system in the tunnel, and the evacuation process will be affected by a thick smoke layer, and smoke control is challenging. Therefore, employing point-extraction system associates with the smoke layer thickness reduction. Considering Figures 4(a) and 4(b), it is observed that for critical velocity (L.V. = 0.53), the lowest smoke back-layering length occurs when there is no extraction point. Considering Figures 4(a) and 4(b), when L.V. = 0.53 m/s and E.V. = 3 m/s, it is observed that the point-extraction system does not operate properly and the extraction point drags the smoke towards itself, and its adverse impact is obvious.

Figure 5 displays the vertical temperature 1 m away from the fire source. It may be perceived that the vertical temperature contour is strongly swayed by both the longitudinal ventilation and ceiling extraction. It is obvious that

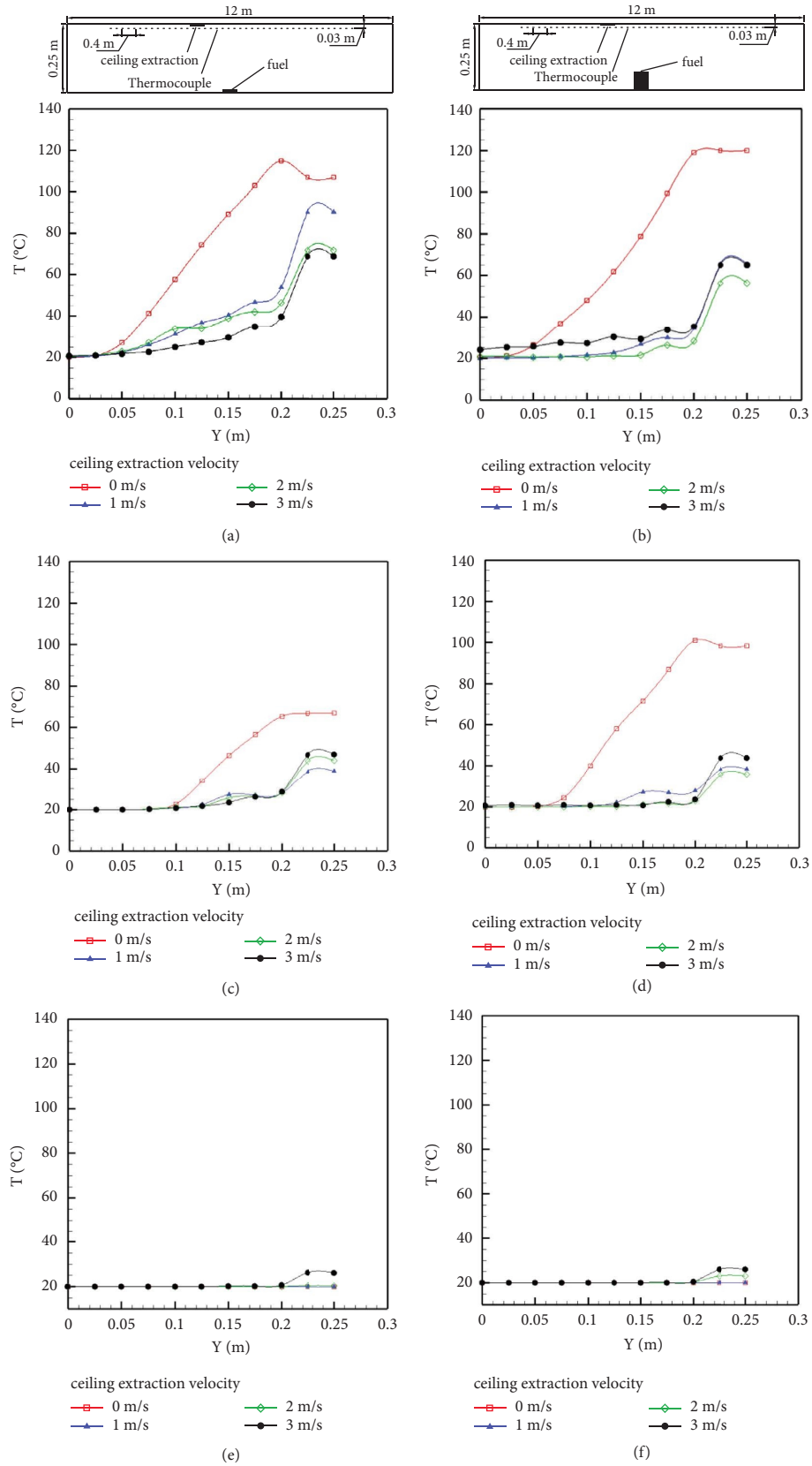

Figure 5: The variation of temperature under the extraction point (HRR = 5 kW with various L.V. (a) L.V. = 0.133 m/s. (b) L.V. = 0.133 m/s. (c) L.V. = 0.265 m/s. (d) L.V. = 0.265 m/s. (e) L.V. = 0.53 m/s. (f) L.V. = 0.53 m/s.

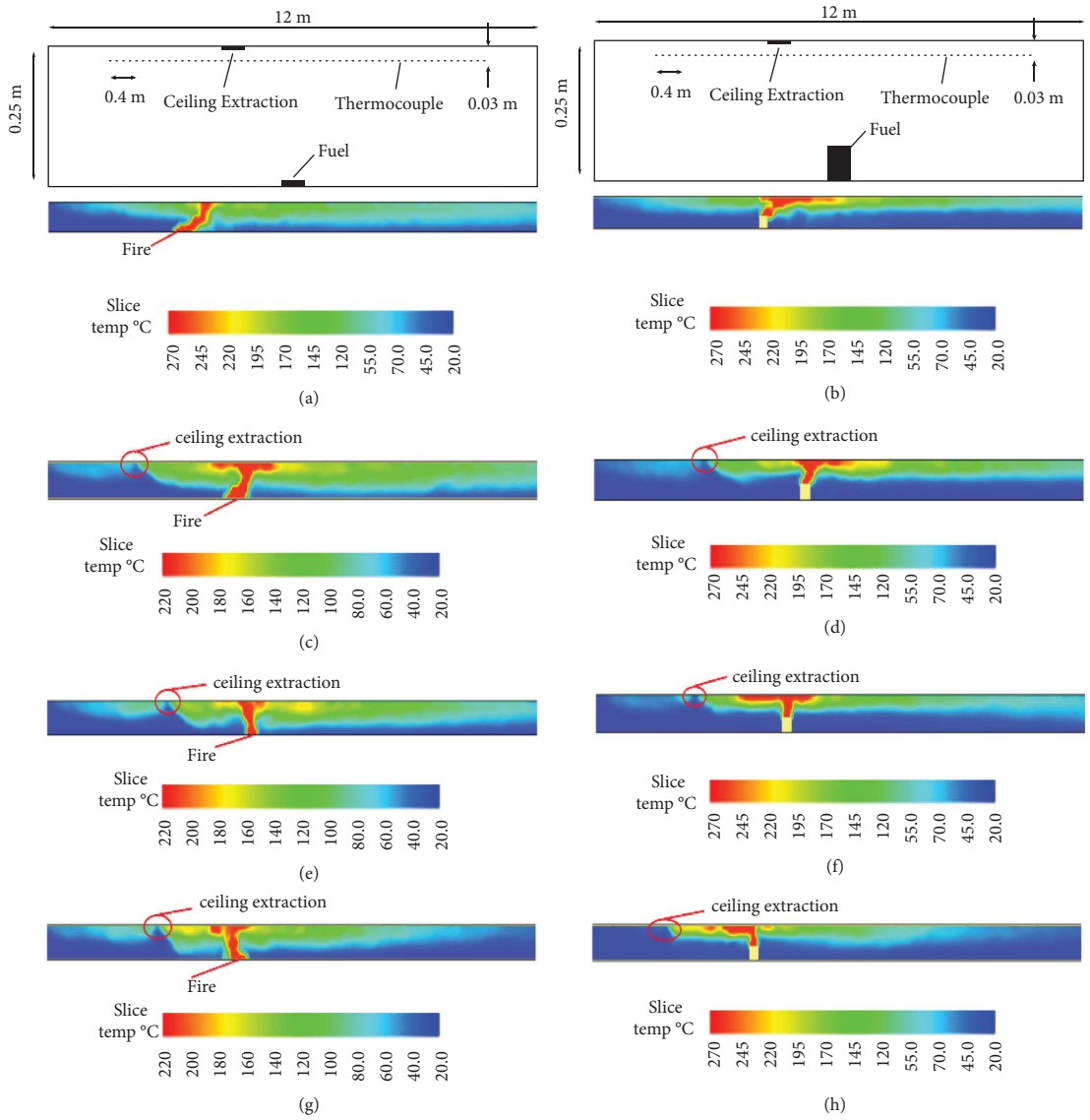

Figure 6: Temperature distribution in a tunnel with various extraction velocities (HRR = 5 kW, L.V. = 0.265 m/s, with various E.V.). (a) Without extraction. (b) Without extraction. (c) E.V. = 1 m/s. (d) E.V. = 1 m/s. (e) E.V. = 2 m/s. (f) E.V. = 2 m/s. (g) E.V. = 3 m/s. (h) E.V. = 3 m/s.

employing the ceiling extraction corresponds to a decrease in vertical temperature profiles. It is worth mentioning as the longitudinal ventilation becomes stronger, the operating of ceiling extraction induces adverse effects. From Figure 5, it is obvious that occurring fire at the height of 0.125 m results in undergoing the higher temperature distribution for E.V. = 0, and combining longitudinal ventilation and point-extraction system associates with enduring lower temperature distribution compared with fire on the floor.

Observing the distribution of the smoke temperature through the tunnel for various extraction velocities is interesting. Figure 6 represents the effects of an extraction velocity on the temperature distribution in the tunnel for L.V. = 0.265 m/s. The plug-holing phenomenon easily occurs when the ceiling mass flow rate increases; subsequently, the lower air layers, fresh air, are drawn into the vent. Apparently, point-extraction system performance will lessen meaningfully when the plug-holing takes place. From Figure 6, it is clear that an increase in ceiling extraction velocity is responsible for the occurrence of plug-holing. From Figure 6(e), it is found that the plug-holing is responsible for the division of the back-layering length into two parts.

Figure 7 illustrates the ceiling temperature distribution when the extraction point is positioned precisely on the fire source. It is evident that elevating the longitudinal ventilation velocity leads to a reduction in the effect of the exhaust vent. Comparison between Figures 3 and 7 reveals that placing the extraction point at 0 meters away from the fire source results in a lower temperature distribution for various extraction velocities. As a consequence, the extraction point at 1 meter away from the fire source does not significantly affect the ceiling temperature distribution compared to the ceiling-fire source distance of 0 meters.

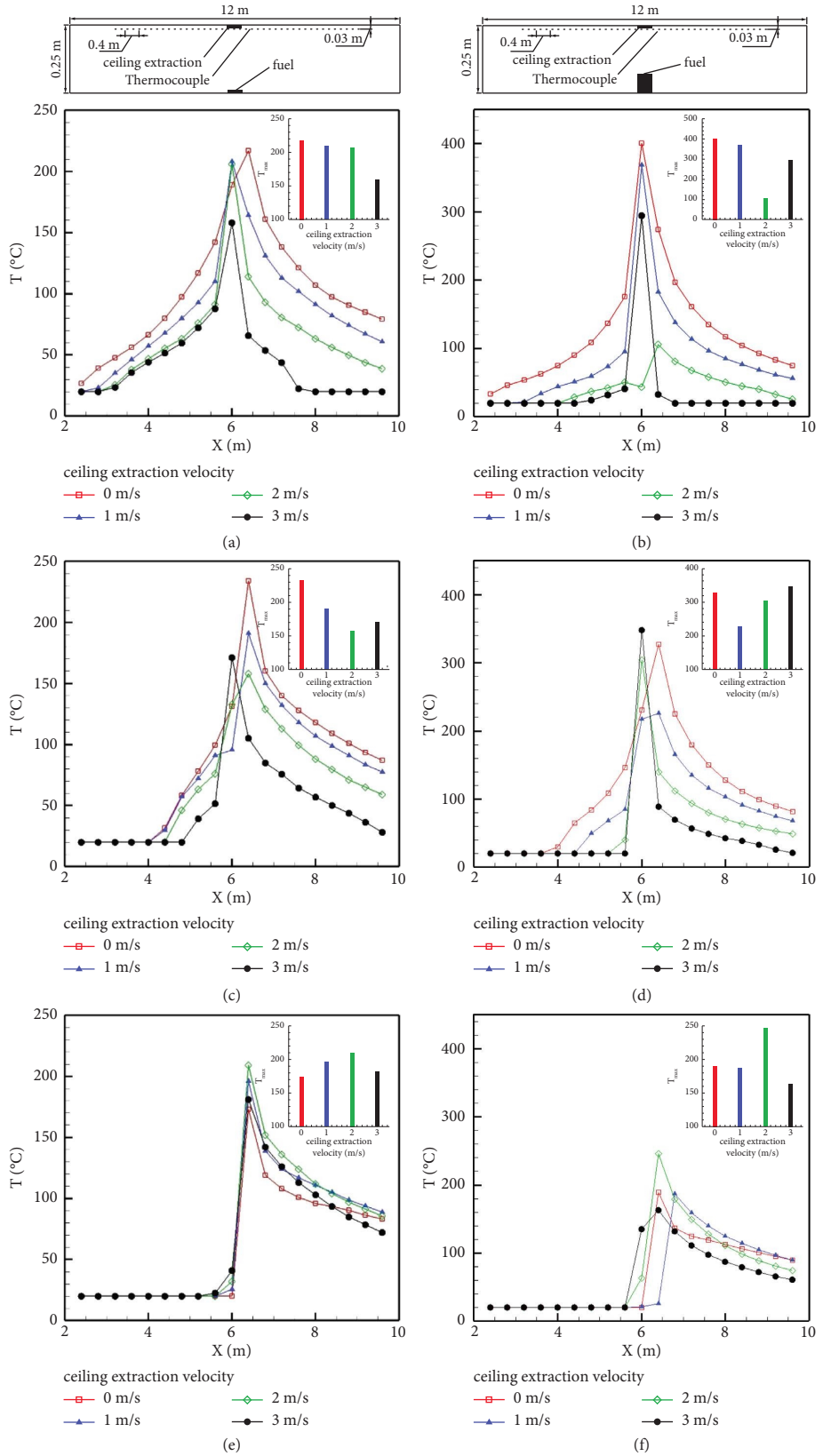

Figure 7: Ceiling temperature distribution through the tunnel with the synergetic effect of ceiling extraction and longitudinal ventilation (HRR = 5 kW with various L.V.). (a) L.V. = 0.133 m/s. (b) L.V. = 0.133 m/s. (c) L.V. = 0.265 m/s. (d) L.V. = 0.265 m/s. (e) L.V. = 0.53 m/s. (f) L.V. = 0.53 m/s.

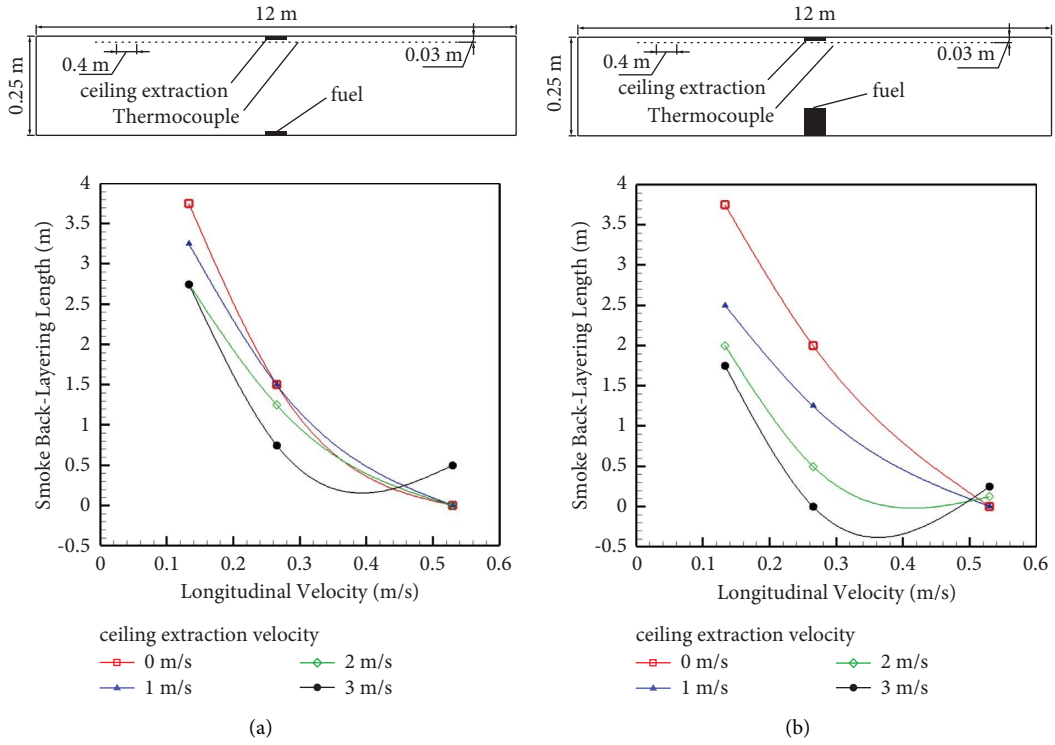

Figure 8: The variation of back-layering flow length with vertical extraction velocity (HRR = 5 kW).

Figure 8 presents the reversed smoke flow length at the upstream of the fire for fires on the floor. It is evident that the extraction velocity and longitudinal ventilation velocity have a noteworthy influence on the back-layering length. As the ceiling extraction velocity reaches 3 meters per second, the back-layering length diminishes to 0 meters. For extraction velocity of 3 m/s and longitudinal velocity of 0.53 m/s, the plug-holing phenomenon occurs, causing a weakening in longitudinal velocity, and consequently, smoke moves towards the upstream side. Thus, the extraction has an unfavorable impact, indicating that the ceiling extraction vent on the fire source drags fresh air instead of smoke.

Figure 9 describes the vertical temperature 0 m away from the fire source. Therefore, the ceiling extraction is not responsible for a decrease in vertical temperature profiles. The development of smoke and plug-holing occurrence in the tunnel are investigated when the longitudinal fire source-extraction distance is 0 m. Figure 10 presents the effects of extraction velocity on the temperature distribution in the tunnel for L.V. = 0.265 m/s. Due to the position of the extraction point, the plug-holing phenomenon does not occur. It is important to mention that abridging the distance between the fire source and vent (1 m to 0 m) benefits shortening the back-layering length.

In a fundamental sense, it is also meaningful to investigate the temperature distribution when the extraction point is settled at the downstream side of the fire source. Figure 11 displays the temperature variations through the tunnel when the extraction opening is placed downstream, and the distance of extraction point and fire source is 1 m. The selection of plans of extraction point position will modify the performance of smoke extraction. When combined longitudinal ventilation and point-extraction system is activated, smoke accumulation will take place just in the vicinity of fire location. Employing the extraction point downstream of the fire is a typical policy to pull smoke off the space beneath the tunnel. It is observed that extraction velocity only influences the ceiling temperature at the downstream side of the fire. Figure 12 displays the stretch of the inverted smoke flow upstream of the fire source, while the extraction point is placed at 1 m away of the fire, concluding that the extraction velocity has no effects on the back-layering length.

Figure 13 describes the variation of ceiling temperature through the tunnel when the distance of extraction point and the fire source is 3 m and the extraction point is placed upstream side (Figure 13(a)) and downstream side (Figure 13(b)) of the fire source. From Figure 13(b), it is clear that extraction velocity does not have an influence on the maximum temperature, but the downside of the fire source experiences lower temperature when the extraction velocity increases. As the distance of fire source and extraction point increases, the influence of extraction on ceiling temperature distribution decreases. Figure 13(a) shows that placing the extraction point 3 m upstream side corresponds to drag the smoke to the upstream side, which has a catastrophic effect on passenger evacuation in the upstream side.

In order to gain a deeper understanding, it is beneficial to determine which factors play more important roles in

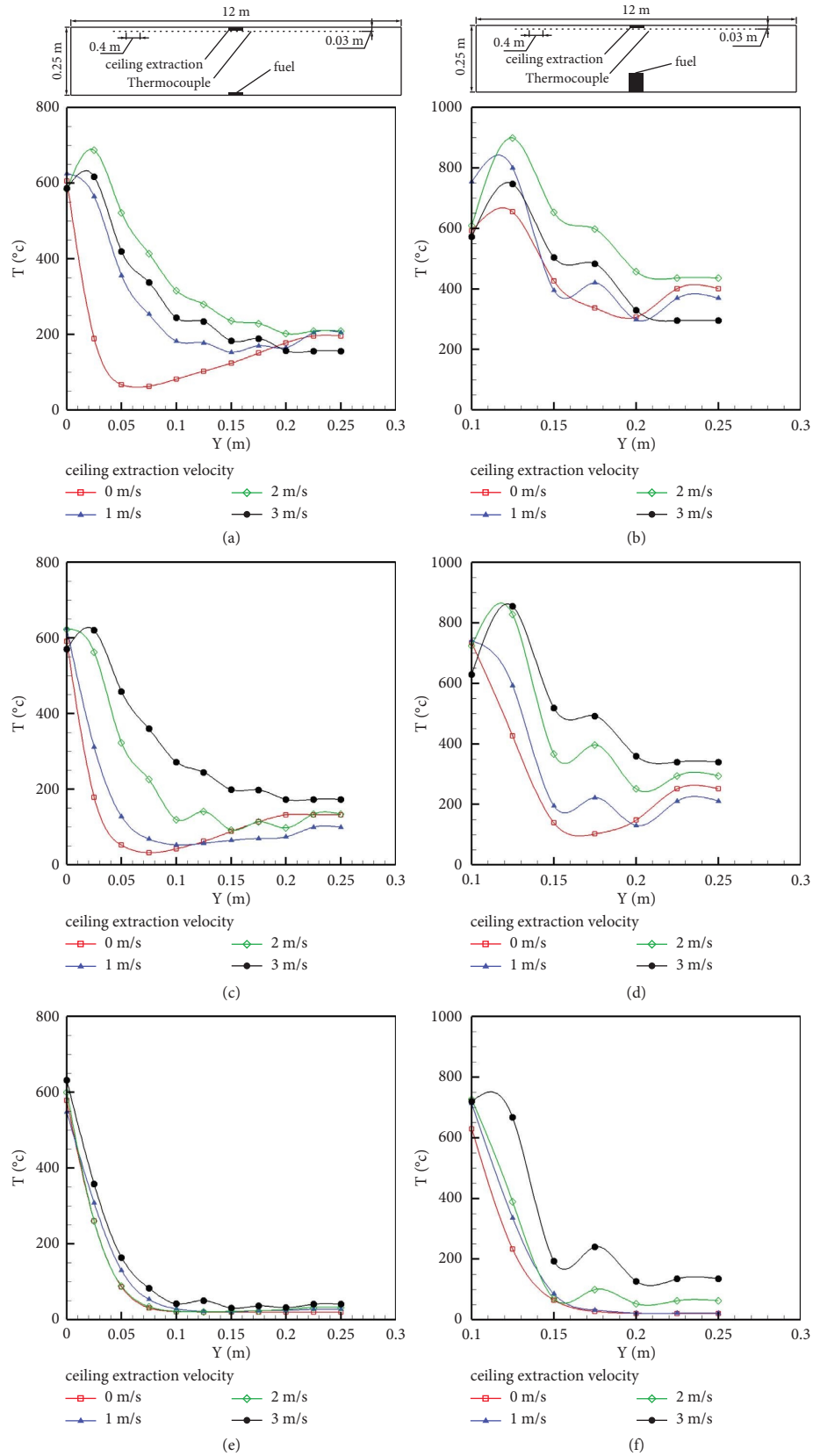

Figure 9: Vertical temperature distribution 0 m away the fire source (exactly under the extraction point, HRR = 5 kW, with various L.V.). (a) L.V. = 0.133 m/s. (b) L.V. = 0.133 m/s. (c) L.V. = 0.265 m/s. (d) L.V. = 0.265 m/s. (e) L.V. = 0.53 m/s. (f) L.V. = 0.53 m/s.

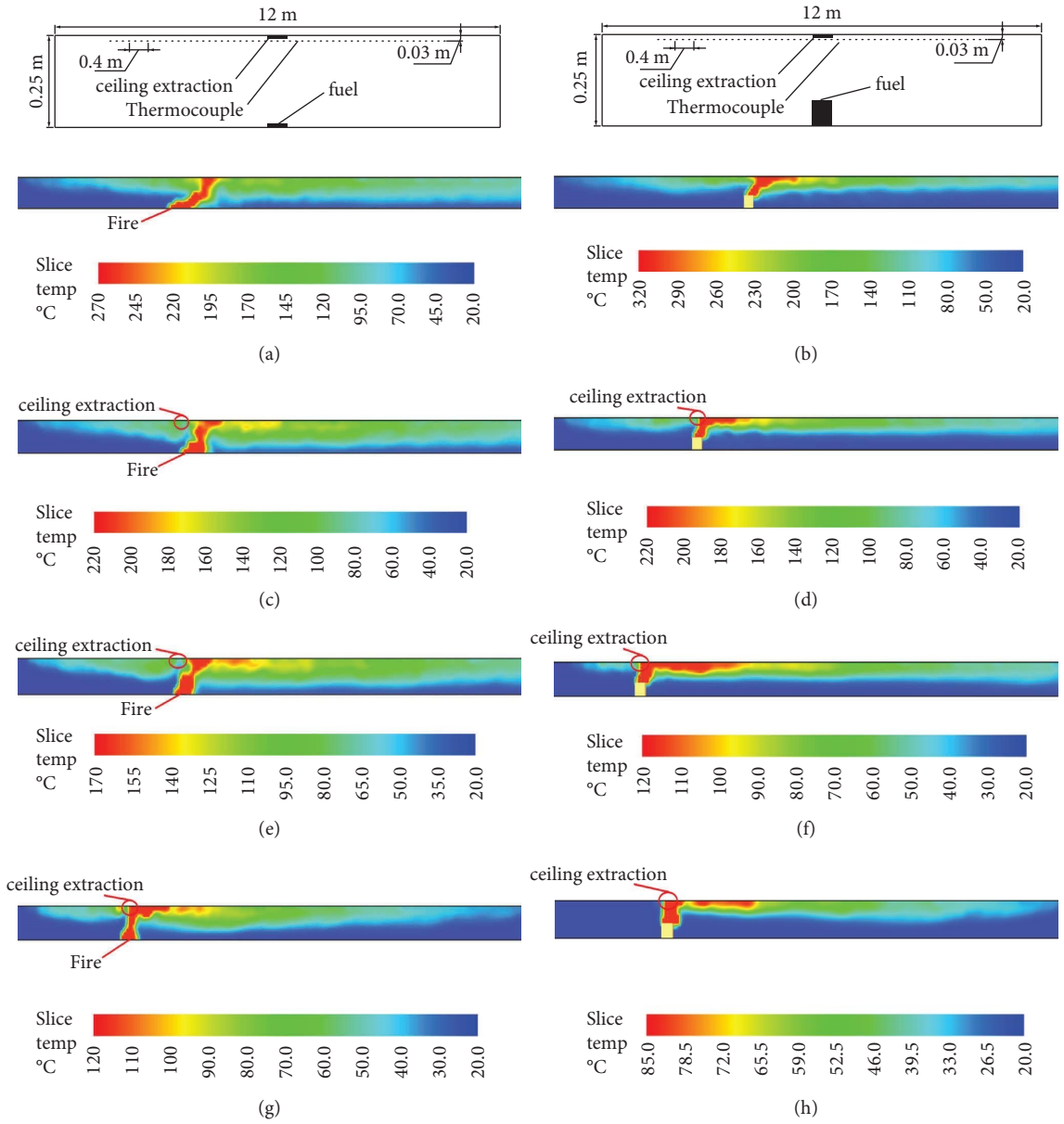

FIGURE 10: Temperature distribution in a tunnel with various extraction velocities (HRR = 5 kW, L.V. = 0.265 m/s, with various E.V.). (a) Without extraction. (b) Without extraction. (c) E.V. = 1 m/s. (d) E.V. = 1 m/s. (e) E.V. = 2 m/s. (f) E.V. = 2 m/s. (g) E.V. = 3 m/s. (h) E.V. = 3 m/s.

controlling the smoke temperature. The Taguchi method is recognized as one of the useful tools for engineers, who can determine the best choices of causes influenced on a phenomenon. In the current work, a $\mathbf{L}_{18}$ orthogonal array is applied, transforming the results into a signal-to-noise ratio (SNR). Signal and noise represent controllable and uncontrollable features in a physical phenomenon, respectively. The first column of Table 1 is dedicated to signals, where the noise is a maximum temperature in the tunnel. With respect to the Taguchi method, the optimal condition links to a situation where the noise factors indicate the least variation of the system performance. Indeed, the situation of the highest SNR introduces the best configuration of the system. Currently, the purpose of optimization is to minimize the maximum temperature of tunnel during a fire. The maximum temperature is considered to be minimized (smaller-better) by the following equation [34, 35]:

$$\mathrm{SNR} = \log_{10}\left(\frac{1}{n}\sum_{i=1}^{n}\left(\frac{1}{y_i}\right)^2\right). \tag{5}$$

Implementing the Taguchi analysis, Table 2 and Figure 14 show the response for signal-to-noise ratios (SNRs) in the situation assumed. The factor with the higher difference between maximum and minimum values of SNR should attach more significance due to its dominant effect. It is obvious that the longitudinal velocity is of paramount which can decrease the maximum temperature; thus,

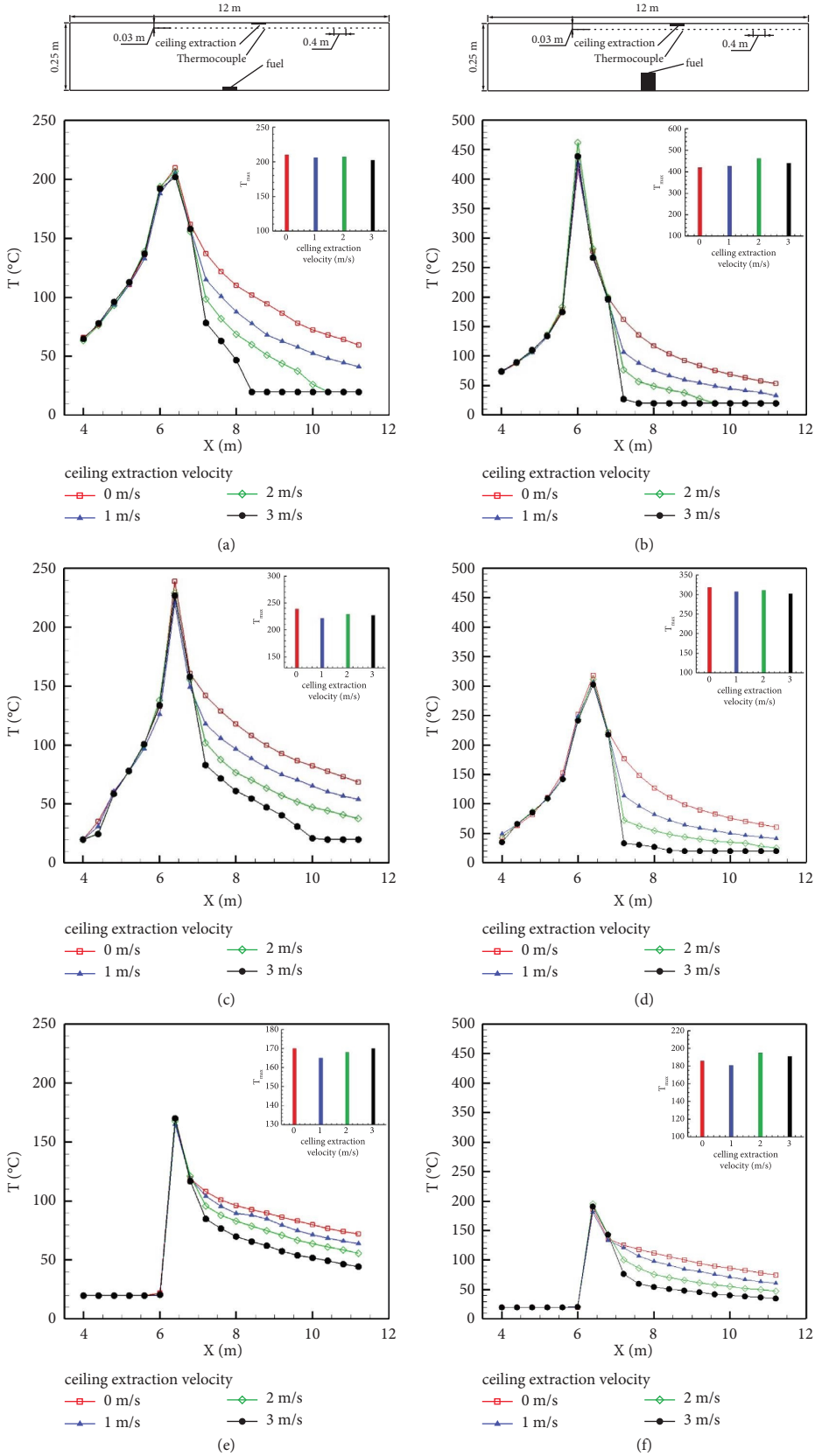

Figure 11: Ceiling temperature distribution through the tunnel with the synergetic effect of ceiling extraction and longitudinal ventilation (HRR = 5 kW with various L.V.). (a) L.V. = 0.133 m/s. (b) L.V. = 0.133 m/s. (c) L.V. = 0.265 m/s. (d) L.V. = 0.265 m/s. (e) L.V. = 0.53 m/s. (f) L.V. = 0.53 m/s.

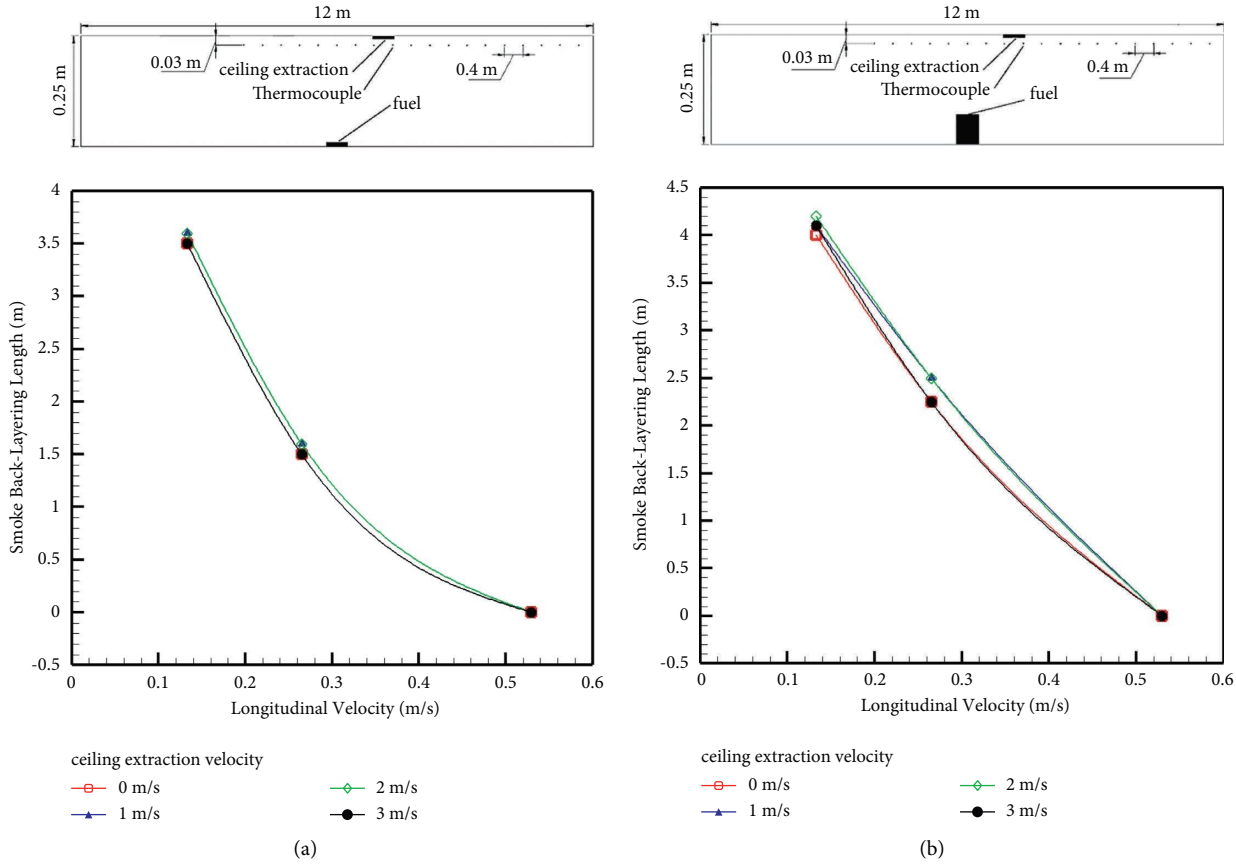

Figure 12: The variation of back-layering flow length with vertical extraction velocity (HRR = 5 kW).

applying the right amount of flow rate can affect a dramatic change in the temperature distribution.

Analysis of variance would be the statistical method employed to clarify data and assist in making the required decisions. In this study, the effectiveness of fire position, longitudinal ventilation system, and exhaust vent system on the extreme temperature in the tunnel can be measured by the exploitation of ANOVA. The P values achieved from the ANOVA indicate that longitudinal ventilation velocity is a more effective parameter in minimizing temperature owing to its minimum P value (see Table 3).

Having implemented ANOVA analysis, a new model for predicting the maximum temperature is proposed. Considering Table 4, each parameter and its coefficient value represent their weight in our suggested model. Equation (6) is a useful tool for predicting the highest temperature for different scenarios, thereby promoting the deeper understanding of this complex problem.

$$\begin{aligned} T\,(\max) = {} & 227.9 + 1987\,\text{height} - 16.7\,\text{distance} - 215\,L.V. - 28.3\,E.V + 16.60\,\text{distance} \times \text{distance} \\ & + 368\,L.V. \times L.V. + 6.66\,E.V \times E.V - 145.8\,\text{height} \times \text{distance} - 4253\,\text{height} \times L.V. \\ & + 94\,\text{height} \times E.V + 150.5\,\text{distance} \times L.V. - 19.99\,\text{distance} \times E.V + 28.2\,L.V. \times E.V. \end{aligned} \tag{6}$$

In Figure 15(a), the highest temperature as a function of longitudinal ventilation velocity and ceiling extraction velocity is illustrated as a contour plot. It is obvious that without applying correct longitudinal ventilation velocity, using the point-extraction system cannot help decrease the highest temperature effectively. Considering Figure 15(b), moving the extraction point from the downstream side of the fire source to upstream should be accompanied by an increase in ceiling extraction velocity to guarantee that the lower temperatures can be experienced in the tunnel. The strong dependence of temperature on the vertical position of fire is depicted in Figure 15(c); meanwhile, longitudinal ventilation velocity is still an applicable tool to decrease the temperature. Indeed, the higher longitudinal ventilation velocity is, the lower the temperature can exist in the tunnel, thereby diminishing the influence of the extraction point position (Figure 15(d)).

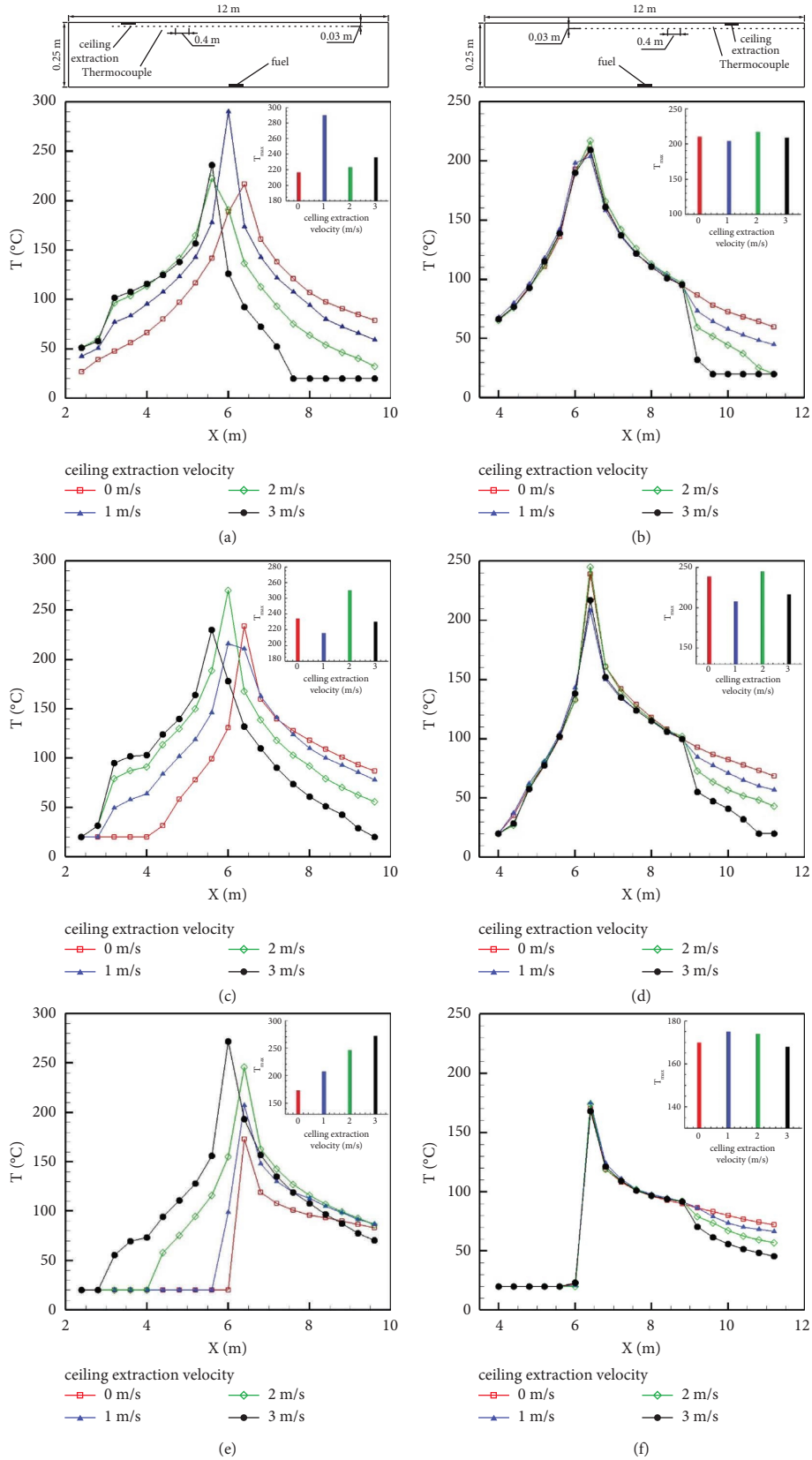

Figure 13: Ceiling temperature distribution through the tunnel with the synergetic effect of ceiling extraction and longitudinal ventilation (HRR = 5 kW with various L.V.). (a) L.V. = 0.133 m/s. (b) L.V. = 0.133 m/s. (c) L.V. = 0.265 m/s. (d) L.V. = 0.265 m/s. (e) L.V. = 0.53 m/s. (f) L.V. = 0.53 m/s.

Table 1: Taguchi table.

Case	Factors				Results
	Height	Distance	H.V.	E.V.	T (max)
1	0	1	0.133	0	218
2	0	1	0.265	1	210
3	0	1	0.53	2	250
4	0	0	0.133	0	220
5	0	0	0.265	1	180
6	0	0	0.53	2	220
7	0	−1	0.133	1	205
8	0	−1	0.265	2	225
9	0	−1	0.53	0	170
10	0.125	1	0.133	2	350
11	0.125	1	0.265	0	320
12	0.125	1	0.53	1	240
13	0.125	0	0.133	1	380
14	0.125	0	0.265	2	300
15	0.125	0	0.53	0	180
16	0.125	−1	0.133	2	460
17	0.125	−1	0.265	0	320
18	0.125	−1	0.53	1	180

Table 2: Factorial effect for the maximum temperature.

Level	Height	Distance	L.V.	E.V.
1	−46.43	−48.29	−49.26	−47.26
2	−49.26	−47.51	−48.06	−47.02
3		−47.73	−46.21	−49.25
Delta	2.83	0.79	3.06	2.24
Rank	2	4	1	3

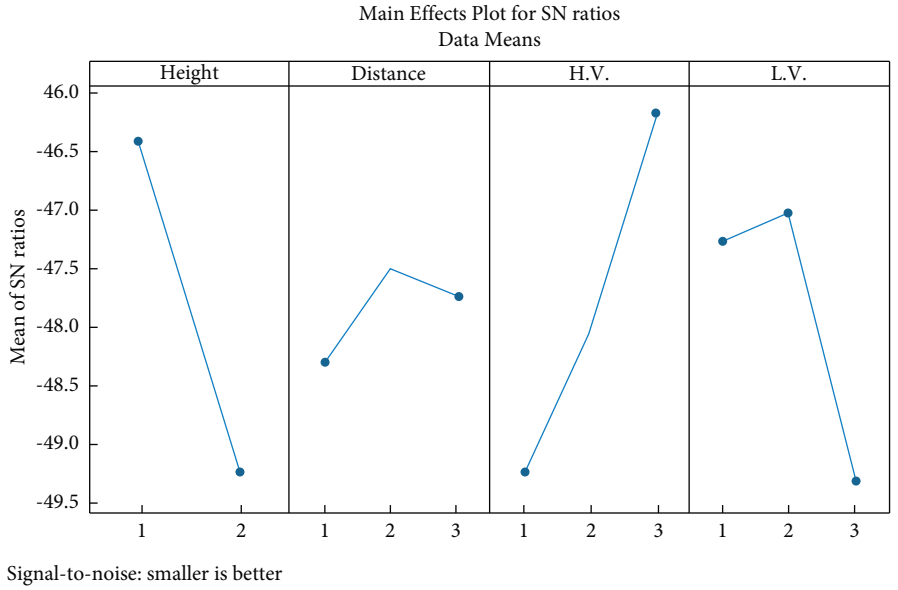

Figure 14: Signal-to-noise ratios for the highest temperature in a tunnel.

5. Future Work

In the case of fire incidents, this study can further explore the use of combined ventilated systems to control temperature distribution and back-layering length, which are critical factors in ensuring the safety of tunnel occupants during fires. Meanwhile, crowd counting and localization can utilize computer vision to analyze crowd scenes in real-time, making it an essential tool for security and public safety personnel [36–38]. Both fields will be employed to ensure people safety to address complex problems in different settings.

Table 3: Coefficients for determining developed model for predicting the maximum temperature.

Source	DF	Adj SS	Adj MS	*F* value	*P* value
Model	13	109565	8428.1	30.68	0.002
Linear	4	39935	9983.7	36.34	0.002
Height	1	22120	22119.8	80.51	0.001
Distance	1	158	157.8	0.57	0.491
L.V.	1	11777	11776.6	42.87	0.003
E.V.	1	1	0.7	0	0.963
Square	3	1755	585	2.13	0.239
Distance × distance	1	1071	1070.6	3.9	0.12
H.V. × H.V.	1	486	485.5	1.77	0.254
E.V. × E.V.	1	140	139.5	0.51	0.515
2-way interaction	6	23423	3903.9	14.21	0.011
Height × distance	1	800	800.3	2.91	0.163
Height × L.V.	1	18114	18113.8	65.93	0.001
Height × E.V.	1	191	191.2	0.7	0.451
Distance × L.V.	1	5071	5071.4	18.46	0.013
Distance × E.V.	1	2209	2209	8.04	0.047
L.V. × E.V.	1	119	118.7	0.43	0.547
Error	4	1099	274.7		
Total	17	110664			

Table 4: Suggested model for predicting the maximum temperature (R_Squared = 99%).

Term	Coded coefficients Coef	SE coef	*T* value	*P* value	VIF
Constant	226.8	12	18.85	0	
Height	41.99	4.68	8.97	0.001	1.43
Distance	4.11	5.43	0.76	0.491	1.29
L.V.	−41.47	6.33	−6.55	0.003	1.82
E.V	0.31	6.11	0.05	0.963	1.63
Distance × distance	16.6	8.41	1.97	0.12	1.03
L.V. × L.V.	14.5	10.9	1.33	0.254	1.36
E.V × E.V	6.66	9.35	0.71	0.515	1.27
Height × distance	−9.11	5.34	−1.71	0.163	1.24
Height × L.V.	−52.76	6.5	−8.12	0.001	1.95
Height × E.V.	5.9	7.08	0.83	0.451	2.19
Distance × L.V.	29.87	6.95	4.3	0.013	1.49
Distance × E.V	−19.99	7.05	−2.84	0.047	1.45
L.V. × E.V.	5.6	8.52	0.66	0.547	2.23

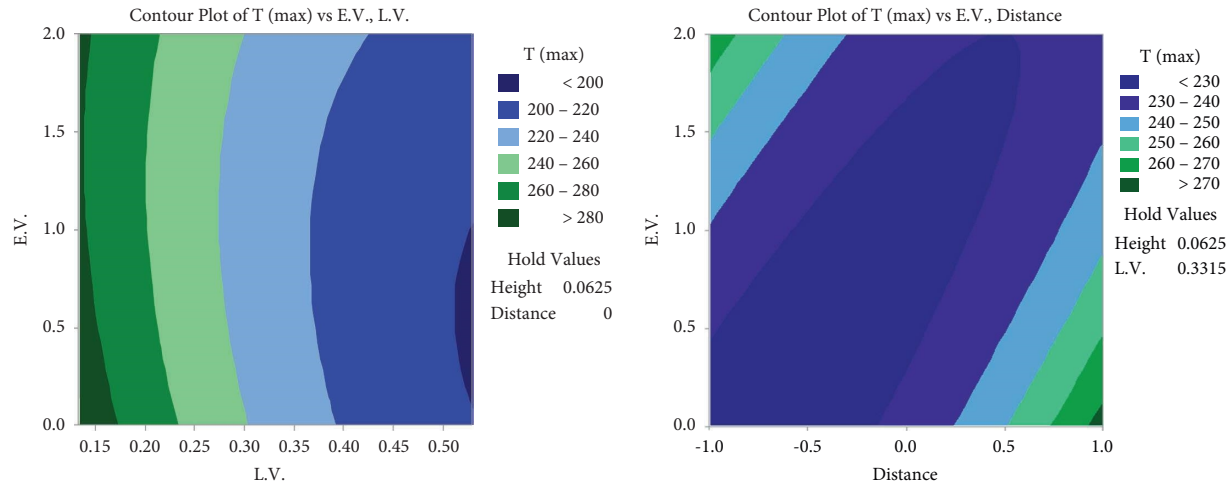

(a) (b)

Figure 15: Continued.

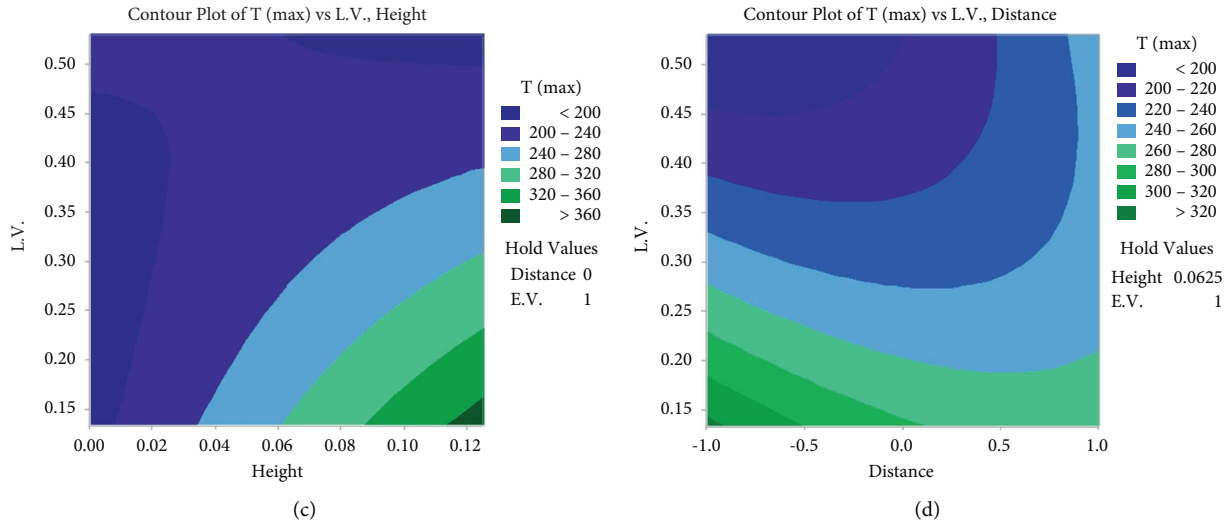

Figure 15: The effect of different factors on the highest temperature in the tunnel.

6. Conclusion

During the course of this investigation, we describe a method for determining the quantity and quality of the temperature distribution when a longitudinal ventilation system is combined with a point-extraction system. In terms of longitudinal ventilation speed, the values of 0.133, 0.265, and 0.53 m/s are set, while the vertical exhaust speed is set at 0, 1, 2, and 3 m/s when the value of heat release rate is 5 kW. A smoke back-layering is generated upstream of the fire source and is controlled by a combination of longitudinal ventilation and point-extraction systems when extraction settles at the upstream side of the fire. Since the fire smoke will be expelled by the vent and blown downstream by the longitudinal ventilation system, it is controlled by the mingled influence of these systems. The foremost outcomes are abridged as follows:

(1) The extraction point has diverse effects provided that the longitudinal ventilation velocity is set by critical velocity

(2) Increment of ceiling extraction velocity and longitudinal ventilation velocity is associated with a reduction in smoke back-layering length

(3) For a fire at a height of 0.125 m, the value of maximum ceiling temperature is 1.8, 1.3, and 1.1 times when the fire source happens on the floor with longitudinal velocities 0.133, 0.265, and 0.53 m/s, respectively

(4) As the fire source-ceiling extraction distance decreases, the possibility of plug-holing decreases

(5) The ceiling extraction is not responsible for decreasing vertical temperature profiles when the longitudinal fire source-ceiling extraction distance is 0 m

By utilizing the Taguchi method, this innovative research aims to investigate the effects of point-extraction systems and longitudinal ventilation on smoke temperature, thermal back-layering length, and plug-holing phenomenon. The study seeks to determine the optimal combination of longitudinal velocity and point-extraction system for ensuring the safe evacuation of people. Furthermore, the proposed equation, which is generated through the Taguchi method, serves as a useful tool for predicting the highest temperature in various scenarios. Through careful examination of essential factors, including ceiling extraction velocity or longitudinal ventilation velocity, the study endeavors to provide valuable insights into these variables and contribute to the current understanding of these phenomena.

Nomenclature

C_P: Specific heat of constant pressure of air mixture ($Jkg^{-1}K^{-1}$)
D^*: The length of the fire scale
D_α: The diffusion coefficient of the α species
f_b: External force ($kg{\cdot}m/s^2$)
G: Gravitational acceleration (m/s^2)
h_s: Sensible enthalpy (J)
$\dot{m}'''_\alpha$: The rate of production of species α (kg/m^3s)
P: Pressure (kg/ms^2)
$\dot{q}'''$: Heat flux vector (kw/m^2)
U: Velocity in the longitudinal direction (m/s)
Y: Mass fraction.

Greek Symbols

ρ: Density (kg/m^3)
τ: Shear stress (kg/m^2)
ε: Energy decay rate (kg/ms^3)
α: Species.

Subscripts

∞: Air conditions
s: Soot.

Data Availability

The data used in this study are available on request from the author.

Conflicts of Interest

The authors declare that they have no conflicts of interest.

References

[1] T. Du, P. Li, and D. Yang, "Downstream stratification of the buoyant contaminants produced by a highly lazy plume in a longitudinally ventilated tunnel," *Building and Environment*, vol. 195, Article ID 107767, 2021.

[2] Z. Long, J. Chen, P. Qiu, and M. Zhong, "Study on the smoke layer height in subway platform fire under natural ventilation," *Journal of Building Engineering*, vol. 56, Article ID 104758, 2022.

[3] H. Miloua, A. Azzi, and H. Y. Wang, "Evaluation of different numerical approaches for a ventilated tunnel fire," *Journal of Fire Sciences*, vol. 29, no. 5, pp. 403–429, 2011.

[4] A. Tanno, H. Oka, K. Kamiya, and Y. Oka, "Determination of smoke layer thickness using vertical temperature distribution in tunnel fires under natural ventilation," *Tunnelling and Underground Space Technology*, vol. 119, Article ID 104257, 2022.

[5] L. Hu, R. Huo, H. B. Wang, and R. X. Yang, "Experimental and numerical studies on longitudinal smoke temperature distribution upstream and downstream from the fire in a road tunnel," *Journal of Fire Sciences*, vol. 25, no. 1, pp. 23–43, 2007.

[6] S. Zhang, Y. Shi, B. Lin et al., "An improved theoretical model for the maximum smoke temperature rise in a tunnel based on equivalent fire source," *Tunnelling and Underground Space Technology*, vol. 122, Article ID 104339, 2022.

[7] P. G. Zhu, X. N. Tong, L. Chen, C. W. Wang, H. Song, and X. Y. Li, "Influence of opening area ratio on natural ventilation in city tunnel under block transportation," *Sustainable Cities and Society*, vol. 19, pp. 144–150, 2015.

[8] C.-S. Ahn, B.-H. Bang, M.-W. Kim, S.-C. James, A. L. Yarin, and S. S. Yoon, "Theoretical, numerical, and experimental investigation of smoke dynamics in high-rise buildings," *International Journal of Heat and Mass Transfer*, vol. 135, pp. 604–613, 2019.

[9] N. Meng, L. Hu, S. Liu, L. Wu, L. Chen, and B. Liu, "Full-scale experimental study on fire suppression performance of a designed water mist system for rescue station of long railway tunnel," *Journal of Fire Sciences*, vol. 30, no. 2, pp. 138–157, 2012.

[10] O. Haghani and E. Barati, "Numerical study on the effect of blower location on the maximum temperature and spread of smoke in case of fire inside tunnels," *Amirkabir Journal of Mechanical Engineering*, pp. 799–802, 2021.

[11] L. Tao and Y. Zeng, "Effect of single-side centralized exhaust on smoke control and temperature distribution in longitudinal ventilation tunnel fires," *Tunnelling and Underground Space Technology*, vol. 119, Article ID 104241, 2022.

[12] Y. F. Wang, X. F. Sun, S. Liu, P. N. Yan, T. Qin, and B. Zhang, "Simulation of back-layering length in tunnel fire with vertical shafts," *Applied Thermal Engineering*, vol. 109, pp. 344–350, 2016.

[13] J. Song, X. Huang, D. Shi, W. E. Lin, S. Fan, and P. F. Linden, "Natural ventilation in London: towards energy-efficient and healthy buildings," *Building and Environment*, vol. 195, Article ID 107722, 2021.

[14] C. Lin and Y. K. Chuah, "A study on long tunnel smoke extraction strategies by numerical simulation," *Tunnelling and Underground Space Technology*, vol. 23, no. 5, pp. 522–530, 2008.

[15] S. Yoon, D. Rie, and H. Kim, "Smoke control of a fire in a tunnel with vertical shaftfire in a tunnel with vertical shaft," *Journal of Loss Prevention in the Process Industries*, vol. 22, no. 6, pp. 954–957, 2009.

[16] H. H. Zhu, Y. Shen, Z. G. Yan, Q. C. Guo, and Q. H. Guo, "A numerical study on the feasibility and efficiency of point smoke extraction strategies in large cross-section shield tunnel fires using CFD modelingfficiency of point smoke extraction strategies in large cross-section shield tunnel fires using CFD modeling," *Journal of Loss Prevention in the Process Industries*, vol. 44, pp. 158–170, 2016.

[17] F. Z. Mei, F. Tang, X. Ling, and J. S. Yu, "Evolution characteristics of fire smoke layer thickness in a mechanical ventilation tunnel with multiple point extractionfire smoke layer thickness in a mechanical ventilation tunnel with multiple point extraction," *Applied Thermal Engineering*, vol. 111, pp. 248–256, 2017.

[18] Z. Yan and Y. Zhang, "Numerical study on the smoke control using point extraction strategy in a large cross-section tunnel in fire," *Tunnelling and Underground Space Technology*, vol. 82, pp. 455–467, 2018.

[19] J. Wang, J. Yuan, Z. Fang, Z. Tang, P. Qian, and J. Ye, "A model for predicting smoke back-layering length in tunnel fires with the combination of longitudinal ventilation and point extraction ventilation in the roof," *Tunnelling and Underground Space Technology*, vol. 80, pp. 16–25, 2018.

[20] X. P. Jiang, M. J. Liu, J. Wang, and Y. Z. Li, "Study on induced airflow velocity of point smoke extraction in road tunnel firesflow velocity of point smoke extraction in road tunnel fires," *Tunnelling and Underground Space Technology*, vol. 71, pp. 637–643, 2018.

[21] F. Tang, L. J. Li, F. Z. Mei, and M. S. Dong, "Thermal smoke back-layering flow length with ceiling extraction at upstream side of fire source in a longitudinal ventilated tunnelflow length with ceiling extraction at upstream side of fire source in a longitudinal ventilated tunnel," *Applied Thermal Engineering*, vol. 106, pp. 125–130, 2016.

[22] F. Tang, Z. L. Cao, Z. He, X. Ling, and Q. Wang, "Thermal plume temperature profile of buoyancy-driven ceiling jet in a channel fire using ceiling smoke extractionfile of buoyancy-driven ceiling jet in a channel fire using ceiling smoke extraction," *Tunnelling and Underground Space Technology*, vol. 78, pp. 215–221, 2018.

[23] Y. F. Wang, Y. L. Li, P. N. Yan, B. Zhang, and L. Zhang, "Maximum temperature of smoke beneath ceiling in tunnel fire with vertical shafts," *Tunnelling and Underground Space Technology*, vol. 50, pp. 189–198, 2015.

[24] Y. F. Wang, X. F. Sun, B. Li, T. Qin, S. Liu, and Y. Liu, "Small-scale experimental and theoretical analysis on maximum temperature beneath ceiling in tunnel fire with vertical shafts," *Applied Thermal Engineering*, vol. 114, pp. 537–544, 2017.

[25] S. Zhao, F. Liu, F. Wang, and M. Weng, "Experimental studies on fire-induced temperature distribution below ceiling in a longitudinal ventilated metro tunnel," *Tunnelling and Underground Space Technology*, vol. 72, pp. 281–293, 2018.

[26] Z. Tao, R. Yang, C. Li, Y. Yao, P. Zhang, and H. Zhang, "An experimental study on fire behavior of an inclined ceiling jet

in a low-pressure environment," *International Journal of Thermal Sciences*, vol. 138, pp. 487–495, 2019.

[27] Y. Huang, Y. Li, Q. Bi et al., "Experimental investigation on temperature profile with downstream vehicle in a longitudinally ventilated tunnel," *Experimental Thermal and Fluid Science*, vol. 103, pp. 149–156, 2019.

[28] F. Tang, Z. L. Cao, Q. Chen, N. Meng, Q. Wang, and C. Fan, "Effect of blockage-heat source distance on maximum temperature of buoyancy-induced smoke flow beneath ceiling in a longitudinal ventilated tunnel," *International Journal of Heat and Mass Transfer*, vol. 109, pp. 683–688, 2017.

[29] Y. Yao, X. Cheng, S. Zhang, K. Zhu, H. Zhang, and L. Shi, "Maximum smoke temperature beneath the ceiling in an enclosed channel with different fire locations," *Applied Thermal Engineering*, vol. 111, pp. 30–38, 2017.

[30] F. Tang, Q. He, and L. Chen, "Experimental study on maximum smoke temperature beneath the ceiling induced by carriage fire in a tunnel with ceiling smoke extraction," *Sustainable Cities and Society*, vol. 44, pp. 40–45, 2019.

[31] L. Li, D. Zhu, Z. Gao, P. Xu, and W. Zhang, "A study on longitudinal distribution of temperature rise and carbon monoxide concentration in tunnel fires with one opening portal," *Case Studies in Thermal Engineering*, vol. 28, Article ID 101535, 2021.

[32] Y. Wu and M. A. Bakar, "Control of smoke flow in tunnel fires using longitudinal ventilation systems–a study of the critical velocity," *Fire Safety Journal*, vol. 35, no. 4, pp. 363–390, 2000.

[33] Y. Z. Li, B. Lei, and H. Ingason, "Study of critical velocity and back layering length in longitudinally ventilated tunnel fires," *Fire Safety Journal*, vol. 45, no. 6-8, pp. 361–370, 2010.

[34] E. Barati, M. Rafati Zarkak, and S. Jalali, "Analysis of heat transfer and flow over a rotating cylinder at subcritical Reynolds numbers based on Taguchi method," *Journal of Thermal Engineering*, vol. 9, no. 4, pp. 1–17, 2023.

[35] E. Barati, M. R. Zarkak, and M. Biabani, "Investigating the effect of the flow direction on heat transfer and energy harvesting from induced vibration in a heated semi-circular cylinder," *Ocean Engineering*, vol. 279, Article ID 114487, 2023.

[36] R. Hu, Z. Tang, E. Q. Wu, Q. Mo, R. Yang, and J. Li, "RDC-SAL: r," *Applied Intelligence*, vol. 52, no. 12, pp. 14336–14348, 2022.

[37] A. Sarviha and E. Barati, "Piezoelectric energy harvester for scavenging steady internal flow energy: a numerical investigation," *Journal of the Brazilian Society of Mechanical Sciences and Engineering*, vol. 45, no. 8, p. 398, 2023.

[38] R. Hu, Q. Mo, Y. Xie et al., "AVMSN: an audio-visual two stream crowd counting framework under low-quality conditions," *IEEE Access*, vol. 9, pp. 80500–80510, 2021.